



Published as: *Neuron*. 2011 October 20; 72(2): 330–343.

A cortical substrate for memory-guided orienting in the rat

Jeffrey C. Erlich¹, Max Bialek¹, and Carlos D. Brody^{1,2}

¹Howard Hughes Medical Institute, Princeton Neuroscience Institute and Department of Molecular Biology, Princeton University, Princeton NJ 08544

Abstract

Anatomical, stimulation and lesion data have suggested a homology between the rat frontal orienting fields (FOF, centered at +2 AP, ± 1.3 ML mm from Bregma) and primate frontal cortices such as the frontal or supplementary eye fields. We investigated the functional role of the FOF using rats trained to perform a memory-guided orienting task, in which there was a delay period between the end of a sensory stimulus instructing orienting direction and the time of the allowed motor response. Unilateral inactivation of the FOF resulted in impaired contralateral responses. Extracellular recordings of single units revealed that 37% of FOF neurons had delay period firing rates that predicted the direction of the rats' later orienting motion. Our data provide the first electrophysiological and pharmacological evidence supporting the existence in the rat, as in the primate, of a frontal cortical area involved in the preparation and/or planning of orienting responses.

INTRODUCTION

Behaviors that require the planning and execution of orienting decisions have long been investigated in rodents. A classic example is navigation through mazes (Tolman, 1938; Hull, 1932; Olton and Samuelson, 1976). Recordings from the rodent hippocampus and entorhinal cortex have led to important discoveries about the neural encoding of navigation and the representation of space (McNaughton et al., 2006; Moser et al., 2008). Navigation is composed of a sequence of individual orienting motions, but in contrast to rodent studies of spatial navigation, the neural control of individual orienting motions has been studied most thoroughly in primates, specifically with regard to the control of gaze by the frontal and supplementary eye fields (FEF and SEF) (Schall and Thompson, 1999; Schiller and Tehovnik, 2005). As a result of being separated by both different model species and by different behavioral paradigms, literatures for the navigation and the orienting systems have remained far apart, making few references to each other (but see Arbib, 1997; Corwin and Reep, 1998; Kargo et al., 2007). Yet the two systems must necessarily interact (Whitlock et al., 2008). As part of bridging the gap between these two fields of research, we took a classic primate behavioral paradigm, memory-guided orienting (Gage et al., 2010; Funahashi et al., 1991), which is known to be FEF-dependent (Bruce and Goldberg, 1985; Bruce et al., 1985),

© 2011 Elsevier Inc. All rights reserved.

²To whom correspondence should be addressed .

Publisher's Disclaimer: This is a PDF file of an unedited manuscript that has been accepted for publication. As a service to our customers we are providing this early version of the manuscript. The manuscript will undergo copyediting, typesetting, and review of the resulting proof before it is published in its final citable form. Please note that during the production process errors may be discovered which could affect the content, and all legal disclaimers that apply to the journal pertain.

SUPPLEMENTAL INFORMATION

Supplemental Information includes seven figures and three movies, as well as Supplemental Experimental Procedures.

and adapted it to rats. Then, in rats performing the task, we studied a rat cortical area that has long been suggested as homologous to the primate FEF.

The area we studied appears in the literature under a large variety of names. These include M2 (Paxinos and Watson, 2004), anteromedial cortex (Sinnamon and Galer, 1984), dorsomedial prefrontal cortex (Covey and Bozek, 1974), medial precentral cortex (Leichnetz et al., 1987), Fr2 (Zilles, 1985), medial agranular cortex (Donoghue and Wise, 1982; Neafsey et al., 1986), primary whisker motor cortex (Brecht et al., 2004), and rat frontal eye fields (Neafsey et al., 1986; Guandalini, 1998). A theme common to many studies of this area, and shared with the primate FEF, is a role in guiding orienting movements. We targeted a particular point at the center of the areas investigated in the studies cited above (+2 AP, ± 1.3 ML mm from Bregma), and refer to the cortex around this point as the frontal orienting field (FOF).

The homology between rat FOF and primate FEF was first proposed four decades ago by C.M. Leonard (1969), based on the anatomical finding that the FOF, like the FEF, receives projections from the mediodorsal nucleus of the thalamus (Reep et al., 1984), and projects to the superior colliculus (SC; Reep et al., 1987). Later, Stuesse & Newman (1990) found that the rat FOF also projects to other oculomotor centers in the rat's brainstem, in a pattern that mimics the oculomotor brainstem projections of the primate FEF. Also like the FEF, the FOF receives inputs from multiple sensory cortices, including visual, auditory, and somatosensory cortices (Conde et al., 1995), and has strong reciprocal connections with the prefrontal (Conde et al., 1995) and parietal cortices (Corwin and Reep, 1998). The rat FOF, like the primate FEF, is thus well-placed to integrate information from many different sources in the service of guiding orienting motions. Leonard's proposal led to studies that found that unilateral lesions of the FOF produced effects consistent with contralateral neglect (Covey and Bozek, 1974; Crowne and Pathria, 1982; Crowne et al., 1986), which is a classic symptom of FEF damage in humans and monkeys (Ferrier, 1875; Hebb and Penfield, 1940). Further support for Leonard's proposal came from studies that revealed orienting motions in response to intracortical microstimulation of the FOF (Sinnamon and Galer, 1984). This parallels the orienting motions produced by stimulation of the primate FEF in head-fixed (Bruce et al., 1985) as well as head-free animals (Monteon et al., 2010). Neafsey et al. (1986) reported that stimulation of the FOF in anesthetized, head-fixed rats produced both eye and whisker motions and suggested it was an eye-head orientation cortex, homologous to the FEF. More recently, based on the whisker motions evoked by electrical stimulation of the FOF, the area has been studied as a whisker motor cortex (Brecht et al., 2004), with particular attention paid to its role in vibrissal active sensing (reviewed in Kleinfeld et al., 2006).

To our knowledge, there are only a few electrophysiological studies recording single neurons of awake animals in this area (we are aware of only three, Carvell et al., 1996; Kleinfeld et al., 2002; Mizumori et al., 2005), and they have not focused on the FOF's role in orienting motions. Kleinfeld (2002) used head-fixed rats, precluding the study of head- or body-orienting movements. Carvell et al. (1996) recorded from awake rats that were whisking freely while being held in the experimenter's hands, but orienting movements were not recorded, and the rats were not required to perform any task. Mizumori et al. (2005) reported head direction tuning (Taube, 2007) in the FOF. Mizumori et al. also mentioned observing neurons that encoded egocentric motions, including orienting movements, but they did not elaborate on this observation.

To further investigate the role of the FOF in the control of orienting, we carried out unilateral pharmacological inactivations of the FOF and recorded extracellular neural spiking signals from the FOF, while rats were performing a memory-guided orienting task

(Gage et al., 2010; Funahashi et al., 1991). Our findings provide the first pharmacological and electrophysiological evidence that the FOF plays an important role in the preparation (Riehle and Requin, 1993) of orienting movements.

RESULTS

The memory-guided orienting task

We developed a computerized protocol to train rats to perform a two-alternative forced-choice memory-guided orienting task (Figure 1A). Training took place in a behavior box with 3 nose ports arranged side-by-side along one wall, and with two speakers, placed above the right and left nose ports. Each trial began with a visible light-emitting diode (LED) turning on in the center port. In response to this, rats were trained to place their noses in the center port, and remain there until the LED was turned off. We refer to this period as the “nose in center” or “fixation” period, and varied its duration randomly from trial to trial (range: 0.9 to 1.5 sec). During the fixation period, an auditory stimulus, consisting of a periodic train of clicks, was played for 300 ms. Click rates greater than 50 clicks/sec indicated that a water reward would be available on the left port; click rates less than 50 clicks/sec indicated that a water reward would be available on the right port. On “memory trials,” the click train was played shortly after the rat placed its nose in the center port, and was followed by a silent delay period before the fixation period ended and the animal was allowed to make its response. On “non-memory trials,” the click train ended at the same time as the fixation period, and the animal could respond immediately after the end of the stimulus. The two types of trials were randomly interleaved with each other in each session. For animals in behavioral and pharmacological experiments, we also interleaved, across trials within each session, six different click rate values, ranging from easy trials, with click rates far from 50 clicks/sec, to difficult trials, with click rates close to 50 clicks/sec. To maximize the number of identically prepared trials, animals in electrophysiological experiments were presented with only two click rates, 100 and 25 clicks/sec, again randomly interleaved across trials (Figure 1C, **filled circles**).

Here we present data from 25 male Long-Evans rats, 5 of which were implanted with bilateral FOF cannula for infusions, 4 of which were implanted with bilateral M1 cannula, and another 5 of which were implanted with microdrives for tetrode recording. Four of the five tetrode-implanted rats performed memory-guided click rate discrimination, as described in Figure 1. As a preliminary test of the effects of a different class of instruction stimulus, the fifth tetrode-implanted rat was trained on a memory-guided spatial location task, in which the click train rate was always 100 clicks/sec, and the rewarded side was indicated by playing the click train from either the left or the right speaker. The behavioral performance and physiological results were similar for the two stimulus classes (i.e., click rate discrimination and location discrimination; see Figure S4), and are reported together in the main text.

Rats performed about 300 trials per 1.5 hour session each day, 7 days a week, for 6 months-1.5 years. After each animal was fully trained, an average of ~66,000 trials per rat were collected. Maintaining fixation is likely to require inhibitory control (Narayanan and Laubach, 2006; Munoz and Wurtz, 1992), and individual rats varied in the percentage of trials in which they broke fixation (range: 10-50%). There were consistently more broken fixation trials for memory trials (mean \pm se, 37 \pm 2%) than for non-memory trials (mean \pm se 29 \pm 2%, paired *t*-test, $p < 10^{-5}$). Unless otherwise specified, all trials where rats prematurely broke fixation were excluded from analyses.

For each rat, we combined the data across sessions and fitted 4-parameter logistic functions to generate one psychometric curve for memory trials, and another curve for non-memory

HHMI Author Manuscript

HHMI Author Manuscript

HHMI Author Manuscript

trials (Figure 1C, thin lines). Percent correct on the easiest memory trials was similar to the easiest non-memory trials (94% vs 95%, paired *t*-test, $p>0.49$). Click frequency discrimination ability, as assayed by the slopes of the psychometric fits at their inflection point, was also similar for memory and non-memory trials (-2.3 vs -2.1% went-right per click/sec, paired *t*-test, $p>0.35$). This suggests that the two types of trials are of similar difficulty.

We tested whether whisking played a role in performance of the memory-guided orienting task in three ways. First, we cut off the whiskers of 3 rats bilaterally. This manipulation had no statistically significant effect on psychometric function slopes or endpoints, although it did produce a small effect on overall percent correct performance ($83\pm 1\%$ without whiskers vs $87\pm 1\%$ with whiskers, *t*-test, $p<0.05$). There was no differential effect on memory vs non-memory trials (*t*-test, $p>0.5$; Figure 1D,F). Second, we probed whether asymmetric whisking played a role in task performance by using unilateral subcutaneous lidocaine injections to temporarily paralyze the whiskers on one side of the face of 4 rats. This manipulation did not generate any lateralized effects on performance, but led instead to a small bilateral effect, indistinguishable from that of bilateral whisker trimming (Figure 1E,F). Third, we performed video analysis of regular sessions (no drug, no whisker trimming), searching for differences in delay period whisking preceding leftwards vs rightwards movements. No significant differences were found (Figure S1). Furthermore, in the video analyzed, the whiskers were held still during the memory delay period (Movie S2, compare to exploratory whisking in Movie S1 and out-of-task whisking Movie S3). In sum, whisking appears to play a negligible role in the memory-guided orienting task.

Muscimol inactivation of the FOF generates a contralateral impairment

In contrast to the negligible effects found from manipulating the whiskers themselves, we found that manipulating neural activity in the FOF produced strong effects on memory-guided orienting. Unilateral inactivation of the FOF generated a clear impairment on trials where the animal was instructed to orient contralateral to the infusion site. (Figure 2, Contra trials). Performance on ipsilaterally-orienting trials was unaffected (Figure 2, Ipsi trials). Contralateral impairment was observed for both memory and non-memory trials, which were randomly interleaved with each other. However, the effect was markedly stronger on memory trials (Figure 2A; compare top row to bottom row). Left infusions impaired rightwards-instructed trials to the same degree that right infusions impaired leftwards-instructed trials (four *t*-tests: contra/mem $p>0.5$, contra/non-mem $p>0.26$, ipsi/mem $p>0.1$, ipsi/non-mem $p>0.4$). We therefore combined data from left and right infusion days for an overall population analysis, and confirmed that performance was worse for contralateral memory trials than non-memory trials (Figure 2B, permutation test $p<0.001$). Since memory and non-memory trials are of similar difficulty (see above), the greater impairment on memory trials suggests that, in addition to a potential role in direct motor control of orienting movements, there is a memory-specific component to the role of the FOF.

To test whether unilateral inactivation of primary motor cortex could produce a similar effect to inactivation of the FOF, we repeated the experiment, in the neck region of M1 [$+3.5$ AP, $+3.5$ ML]. This is the same region in which Gage et al. (2010) recorded single-units during a memory-guided orienting task. Unilateral muscimol in M1 produced a pattern of impairment that was different, and much weaker, than that produced in the FOF. In particular, we found no difference in the impairment of contra-memory versus ipsi-memory trials (*t*-test, $p>0.35$) (Figure S2A-D).

Neurons in the FOF prospectively encode future orienting movements

We obtained spike times of 242 well-isolated neurons from five rats performing the memory-guided orienting task. No significant differences were found across recordings from the left and right sides of the brain. Accordingly, we grouped left and right FOF recording data together. Below we distinguish between trials in which animals were instructed to orient in a direction opposite to the recorded side (“contralateral trials”) and trials in which they were instructed to orient to the same side (“ipsilateral trials”).

We first analyzed spike trains from correct trials, with a particular interest in cells that had differential contra versus ipsi firing rates during the delay period, i.e., after the end of the click train stimulus but before the Go signal (see Figure 1A). We identified such cells by obtaining the firing rate from each correct trial, averaged over the entire delay period, and using ROC analysis (Green and Swets, 1974) to query whether the contra and ipsi firing rate distributions were significantly different. By this measure, we found that 89/242 (37%) of cells had significantly different contra versus ipsi delay period firing rates (permutation test, $p < 0.05$). We refer to these cells as “delay period neurons.” Examples of single-trial rasters for 6 delay period neurons are shown in Figure 3.

For each cell, we then took the spike train from each trial and smoothed it with a half-Gaussian kernel to produce an estimated firing rate as a function of time (s.d. of whole Gaussian=200 ms; smoothing process is causal, i.e., looks only backwards in time). At each timepoint, this gave us, across trials, a distribution of firing rates on contralateral trials and a distribution of firing rates on ipsilateral trials. We used ROC analysis to query whether the distributions were significantly different at each timepoint. By this assay, we found that (113/242) (47%) of cells in the FOF had significantly different contra versus ipsi firing rates at some point in time during memory trials (overall probability that a cell was labeled as significant by chance $p < 0.05$; time window examined ran from -1.5 sec before to 0.5 sec after the Go signal).

The temporal dynamics of delay period neurons were quite heterogenous. Different cells had significantly different contra versus ipsi firing rates at different timepoints during the trial (indicated for each cell in Figure 3 by black horizontal bars). At each timepoint, we counted the percentage of neurons, out of the 242 recorded cells, that had significantly different contra versus ipsi firing rates, and plotted this count as a function of time for memory trials and for non-memory trials (Figure 3C). For memory trials the population first became significantly active at 850 ms before the Go signal (Figure 3C, horizontal orange bar). For non-memory trials the population became active 120 ms before the Go signal (Figure 3C, horizontal green bar). At the time of the Go signal on memory trials, 28% of cells had firing rates that predicted the choice of the rat.

We labeled cells as “contra preferring” if they had higher firing rates on contra trials, and as “ipsi preferring” if they had higher firing rates on ipsi trials. When firing rates were examined across time (from -1.5 secs before to 0.5 secs after the Go signal), most cells had a label that was consistent across the duration of the trial: 82/89 (92%) of significant delay period neurons were labeled exclusively as either contra-preferring or ipsi-preferring. Seven of the 89 (8%) delay period neurons switched preference at some point during the trial, usually between the delay period and late in the movement period (data not shown). For our analyses below, we used labels based on the average delay period firing rate.

Given the strong difference in contralateral versus ipsilateral impairment during unilateral inactivation (Figure 2), we were surprised to find no significant asymmetry in the number of contra-preferring versus ipsi-preferring delay period neurons: 50/89 cells (56%) fired more on contralateral trials (three examples are shown in Figure 3A), while 39/89 (44%) fired

more on ipsilateral trials (three examples in Figure 3B). Although there were slightly more contra preferring cells, the difference in number of contra vs ipsi-preferring cells was not statistically significant (χ^2 test on difference, $p>0.2$).

To perform population analyses of firing rates, we first z-score normalized each cell's perievent time histograms (PETHs) by subtracting their mean and dividing by their standard deviation, and then averaged across cells to obtain population normalized PETHs, shown in Figure 4A-D. The early onset ramp we found in the count of cells with significantly different contra versus ipsi memory trial firing rates (orange line, Figure 3C) is paralleled in Figures 4A,B by an early onset in population firing rate difference for contra versus ipsi memory trials. Similarly, the late onset ramp in Figure 3C for non-memory trials is paralleled in Figures 4C,D.

We then turned to analyzing error trials. The activity on error trials (shaded pink for ipsi-instructed but contra motion, and blue for contra-instructed but ipsi motion, Figure 4A-D) showed that, on average across the population, cells that fire more on correctly performed contra-instructed trials also fire more on erroneously performed ipsi-instructed trials; that is, these cells fire more on trials where the animal orients contralateral to the recorded side, regardless of the instruction. Similarly, ipsi preferring cells fire more on trials where the animal orients ipsilaterally, regardless of the instruction. This indicates that the firing rates of FOF cells are better correlated with the subject's future motor response than with the instructing sensory stimulus. We quantified this observation on a cell-by-cell basis by generating a Side-Selectivity Index for each neuron (SSI, see Experimental Procedures for details). Positive SSIs mean that a cell fired more on contra-instructed trials. Negative SSIs mean that a cell fired more on ipsi-instructed trials. If cells encode the instruction we would expect $SSI_{\text{correct}} \approx SSI_{\text{error}}$. But if cells encode the direction of the motor response, then we would expect $SSI_{\text{correct}} \approx -SSI_{\text{error}}$. We first calculated the SSI focusing on the delay period of memory trials. We found that, over neurons, SSI_{correct} correlates negatively with SSI_{error} ($r=-0.42$, $p<10^{-4}$), confirming that on memory trials, the delay period firing rates of FOF neurons encode the orienting choice of the rat, not the instruction stimulus. We then repeated this calculation for firing rates over the movement period (from Go signal to 0.5 sec after the Go signal), for both memory (SSI_{correct} and SSI_{error} correlation $r=-0.59$, $p<10^{-8}$) and non-memory ($r=-0.78$, $p<10^{-17}$) trials. These negative correlations indicate that the FOF is again encoding the motor choice of the rat. We summarized the observations from both the delay and movement periods by calculating the SSI for the entire period, from -1.5 sec before to 0.5 sec after the Go cue. This again resulted in negative SSI_{correct} and SSI_{error} correlations for both memory ($r=-0.49$, $p<10^{-5}$) and non-memory ($r=-0.59$, $p<10^{-8}$) trials (Figure 4E). Overall, then, the firing rates of FOF neurons encode the orienting choice of the rat, not the instruction stimulus.

If the delay period activity in the FOF subserves the planning of an orienting movement, then variation in that activity should lead to variation in behavior, even when the instruction stimulus is held constant (Riehle and Requin, 1993). One measure of trial-to-trial covariation between neuronal signals and choice behavior is Choice Probability (Britten et al., 1996), which quantifies the probability that an ideal observer of the neuron's firing rate would correctly predict the choice of the subject. We computed the choice probability for firing rates of delay period cells. For each cell, we focused on the last 400 ms of the delay period, using only memory trials in which the instruction was to orient to the cell's preferred side. Consistent with the SSI delay period analysis, we found that an ideal observer would, on average, correctly predict the rat's side port choice 64% of the time. The cell population is strongly skewed above the chance prediction value of 0.5, with 75% of cells having a choice probability value above 0.5 (Figure 4F). Twenty-seven percent of cells had choice

probability values that were, individually, significantly above chance (permutation test, $p < 0.05$).

We used red and blue LEDs, placed on the tetrode recording drive headstages of the electrode-implanted rats, to perform video tracking of the rats' head location and orientation (Neuralynx; MT). Two thirds of the delay period neurons (53/89) were recorded in sessions in which head tracking data was also obtained. Figure 5A shows an example of head angular velocity data for left memory trials in one of the sessions, aligned to the time of the Go signal. There is significant trial-to-trial variability in the latency of the peak angular velocity as the animal responds to the Go signal and turns towards a side port to report its choice. As shown in data from the example cells of Figure 3, and an example cell in Figure 5B, many neurons with delay period responses also fire strongly during the movement period, and the latency of each neuron's movement period firing rate profile can vary significantly from trial to trial. To quantitatively estimate latencies on each trial, we used an iterative algorithm that finds, for each trial, the latency offset that would best align that trial with the average over all the other trials (Figure 5A,B; see Experimental Procedures for details). Firing rate latencies and head velocity latencies were estimated independently of each other using this algorithm. We then computed, for each neuron, the correlation between the two latency estimates (e.g., Figure 5C). We focused this analysis on correct contralateral memory trials of delay period neurons (as in Riehle and Requin, 1993). Out of the 53 delay period cells analyzed, 23 of them (43%) showed significant trial-by-trial correlations between neural and behavioral latency (Figure 5D). Furthermore, as a population, the 53 cells were significantly shifted towards positive correlations (mean \pm s.e. 0.36 ± 0.05 , t -test $p < 10^{-8}$). We concluded that a significant fraction of delay period neurons not only have firing rates that predict the direction of motion before it occurs (Figure 4F), but in addition, once the motion has begun, the timing of their firing rate profile is strongly correlated with the timing of the execution of the movement.

Delay period firing rates cannot be explained as encoding head direction

On memory trials, the subject has many hundreds of milliseconds to plan a motor response in advance of the go signal. We examined the behavioral data for evidence of planning, and found it in two forms: faster reaction times on memory trials, and head angle adjustments during the fixation period. With respect to reaction time, we found that the time from exiting the central port until reaching the side port was, on average, 47 ms shorter on memory trials compared to non-memory trials (t -test, $t_{141} = 3.58$, $p < 10^{-5}$, Figure 6A). This is consistent with the idea that prepared movements take less time to initiate and/or execute.

We then asked whether there were any consistent head direction adjustments during the fixation period that would predict subsequent orienting motion choices. Figure 6B plots $\varphi(t)$, the head angle as a function of time aligned to the Go signal, for both left-orienting and right-orienting trials. As can be seen from the average $\varphi(t)$ for each of these two groups, during the delay period of memory trials, rats tended to gradually and slightly turn their heads towards their intended motion direction, even while keeping their nose in the center port. At the time of the Go signal, $\varphi(t=0)$, the rats' heads had already turned, on average, $\sim 4^\circ$ in the direction of the intended response. We used ROC analysis at each timepoint t to quantify whether the distribution of $\varphi(t)$ for trials where the animal ultimately oriented left was significantly different from the distribution for trials where the animal ultimately oriented right. We found that, on average, $\varphi(t)$ allowed a significantly above-chance prediction of the rat's choice 444 ± 29 ms before the Go signal (mean \pm s.e.) on memory trials, and 19 ± 26 ms before the Go signal on non-memory trials. We also found that on some sessions (8/80, 10%) $\varphi(t)$ was not predictive of choice at any timepoint before the Go signal, even while percent correct performance and neural delay period activity was normal in these sessions. This showed that preliminary head movements were not performed by all rats in all

sessions, and suggested that preliminary head movements may not be necessary for performance of the task.

Firing rates of some neurons in rat FOF have been previously described as encoding head-direction responses (Mizumori et al., 2005). That is, the firing rates of some FOF neurons were a function of the allocentric orientation of the animal's head (Taube, 2007). Our recordings replicated this observation (Figure S6). Our data further revealed that head direction tuning in the FOF was significantly affected by behavioral context: for many cells the preferred direction depended on whether the animal was engaged versus not engaged in performing the task (Figure S6).

Here, the observation of head direction tuning in the FOF, together with the data of Figure 6B, immediately raised the question of whether delay period firing rates could predict the rat's choice merely by virtue of encoding the current head orientation φ (which, as shown in Figure 6B, is itself predictive of the rat's choice). To address this question in a quantitative manner that did not depend on an in-task vs out-of-task comparison or distinction, we took advantage of existing variability in φ during the fixation period. We first re-performed the analysis of Figure 3A, but now restricting it to neurons recorded in sessions where head-tracking data was also recorded. We divided trials into two groups, based on the sign of φ at $t=+0.6$ s after the Go signal (shown in Figure 7A as traces in blue $\varphi(0.6)>0$, and red $\varphi(0.6)<0$). These two groups are essentially identical to the "ultimately went Left" and "ultimately went Right" groups of Figure 6B, but re-defining them in terms of the sign of $\varphi(t)$ will prove convenient below. We counted the percentage of neurons that had firing rates that significantly discriminated between these two $\varphi(0.6)>0$ and $\varphi(0.6)<0$ groups. The result, essentially replicating that of Figure 3A for the subset of sessions with head tracking data, is shown in Figure 7B. At the time of the Go signal ($t=0$), 21% of cells significantly discriminated $\varphi(0.6)>0$ vs $\varphi(0.6)<0$ trials. At this same time point ($t=0$), the mean difference in φ for the two groups of trials was $\sim 8^\circ$. In other words, if FOF firing rates simply encode current head angle, an 8° head direction signal should produce a detectable firing rate change in $\sim 21\%$ of cells. We then performed the same analysis, but this time based on the sign of φ at $t=-0.9$ s before the Go signal (traces in blue for $\varphi(-0.9)>0$, and red for $\varphi(-0.9)<0$ in Figure 7C). At $t=-0.9$ s, the mean difference in φ for this new grouping of trials was $\sim 8^\circ$, very similar to the difference at $t=0$ s for the previous grouping (compare Figure 7A and C). However, only 5% of cells discriminated between the two groups at $t=-0.9$ s (Figure 7D). This is in strong contrast to the 21% that we would have expected if FOF neurons encoded head angle. We concluded that encoding of head angle was not sufficient to explain the FOF delay period firing rates that predict orienting choice. We repeated this analysis with angular head velocity $\varphi'(t)$ (Figure S7A-D), and with angular head acceleration $\varphi''(t)$ (Figure S7E-H) and found that, as with head angle, neither angular head velocity nor angular head acceleration could explain choice-predictive delay period firing rates. We also performed a regression analysis, fitting the firing rate of each cell on each trial, $f(t)$, as a linear function of angular position, velocity, and acceleration ($f(t) = \beta_1\varphi(t) + \beta_2\varphi'(t) + \beta_3\varphi''(t) + r(t)$; see Supplementary Experimental Procedures for details). The residuals $r(t)$ have had any linear effects of head angular position, velocity, and/or acceleration eliminated. At each timepoint, we used ROC analysis to test whether the distributions of residuals $r(t)$ for ipsilateral vs contralateral trials were different, and as in Figure 3C, we counted the number of neurons for which this difference was significant. We found that only a small portion of the delay period activity could be accounted for by a combination $\varphi(t)$, $\varphi'(t)$ and $\varphi''(t)$ (Figure S7I).

DISCUSSION

To investigate the contribution of the rat Frontal Orienting Field (FOF; studies centered at +2 AP, ± 1.3 ML mm from Bregma) to the preparation of orienting motions, we trained rats

on a two-alternative forced-choice memory-guided auditory discrimination task. Subjects were presented with an auditory cue that indicated which way they should orient to obtain a reward. However, the subjects were only allowed to make their motor act to report a choice after a delay period had elapsed. The task thus separates the stimulus from the response in the tradition of classic memory-guided tasks (Mishkin and Pribram, 1955; Fuster, 1991; Goldman-Rakic et al., 1992). We carried out unilateral reversible inactivations of the FOF, M1 and the whiskers, recorded extracellular neural spiking signals from the FOF, and tracked head position and orientation, while rats were performing the task. The resulting data provide several lines of evidence supporting the hypothesis that the FOF plays a role in memory-guided orienting. First, unilateral inactivation of the FOF produced an impairment of contralateral orienting trials that was substantially greater for memory trials as compared to non-memory trials (Figure 2). Control performance on both memory and non-memory trials was very similar (Figure 1 and related text), suggesting that the differential impairment was not due to a difference in task difficulty, but instead reveals a memory-specific role of FOF activity in contralateral orienting. Second, we found robust neural firing rates during the delay period (after the offset of the stimulus and before the Go cue) that differentiated between trials in which the animal ultimately responded by orienting contralaterally from those where it responded by orienting ipsilaterally (Figures 3, 4). Third, we found trial-by-trial correlations between neural firing and behavior, both for firing rates during the delay period (Figure 4H) and for neural response latency during periods that included the subjects' choice-reporting motion. (Figure 5). Several groups studying the neural basis of movement preparation (Riehle and Requin, 1993; Dorris and Munoz, 1998; Steinmetz and Moore, 2010; Curtis and Connolly, 2008) have agreed upon three operational criteria for interpreting neural activity as being a neural substrate for movement preparation: 1) Changes in neural activity must occur during the delay period, before the Go signal; 2) The neural activity must show response selectivity (e.g., fire more for contralateral than ipsilateral responses); 3) There must be a trial-by-trial relationship between neural activity and some metric of behavior (usually reaction time, but since our task was not a reaction time task we used choice probability). Our results satisfy all three of these criteria, so interpreting the activity in the FOF as "movement preparation" is, at least, consistent with prior work. There are several possible interpretations as to what component(s) of response preparation FOF neurons might encode: do they represent a motor plan? a memory of the identity of the motor plan? attention? intention? (Bisley and Goldberg, 2010; Glimcher, 2003; Goldman-Rakic et al., 1992; Schall, 2001; Thompson et al., 2005; Gold and Shadlen, 2001). Our data do not discriminate between these possibilities. Nevertheless, we conclude that, as in the primate, there exists in the rat frontal cortex a structure that is involved in the preparation and/or planning of orienting responses. An area with such a role may be conserved across multiple species, including birds (Knudsen et al., 1995).

Since FOF delay period firing rates are better correlated with the upcoming motor act than with the initial sensory cue (Figure 4), our data do indicate that FOF neurons are not likely to encode a memory of the auditory stimulus itself. Furthermore, in memory trials, some form of memory is required immediately after the end of the auditory instruction stimulus. We did not observe a short-latency sensory response in the FOF, but instead observed a slow and gradual development of choice-dependent activity during the delay period. This suggests that FOF neurons do not support the early memory the task requires. The FOF is strongly interconnected with the posterior parietal cortex (PPC, Reep and Corwin, 2009; Nakamura, 1999) and with the medial prefrontal cortex (mPFC, Conde et al., 1995). We suggest both of these areas as candidates for supporting the early memory aspects of the task, perhaps even including the transformation from a continuous auditory signal (click-rate) to a binary choice (plan-left/plan-right). Based on data from an orienting task driven by olfactory stimuli, Felsen and Mainen (2008) recently proposed that the superior colliculus (SC) may play a broad role in sensory-guided orienting. Projections to the SC from the FOF

(Leonard, 1969; Kunzle et al., 1976; Reep et al., 1987), together with our current data, suggest that the FOF may be an important contributor to orienting-related activity in the SC. As in the primate, orienting behavior in the rodent is likely to be subserved by a network of interacting brain areas. The relative roles and mutual interactions between the FOF, PPC, mPFC, and SC (and possibly other areas, including the basal ganglia) during orienting behaviors in the rat remain to be elucidated.

We focused our analyses here on the response-selective delay period activity of FOF neurons. However, we also found neurons carrying a wide variety of other task related neural signals, including ramping during the delay that was not response-selective (consistent with a general timing or anticipatory signal), sustained firing rate increases or decreases during the fixation period, and activity after the reward/error signal. Detailed descriptions of these neural responses are outside the scope of this manuscript and will be reported elsewhere.

If we think of visual saccades as orienting responses, the results presented here from the rat FOF are, qualitatively speaking, consistent with results from monkey FEF studies of memory-guided saccades. Muscimol inactivation of FEF strongly impairs memory-guided contralateral saccades, but leaves visually guided and ipsilateral saccades relatively intact (Sommer and Tehovnik, 1997; Dias and Segraves, 1999; Keller et al., 2008). Similarly, we found that muscimol inactivation of rat FOF strongly impaired memory-guided contralateral orienting, had a weaker effect on non-memory contralateral orienting, and spared ipsilateral orienting (Figure 2). However, FEF inactivation also increases reaction times of contralateral saccades and increases the rate of premature ipsilateral responses, two results that we failed to replicate. Recordings from monkey FEF show robust spatially selective delay period activity in memory-guided saccade tasks (Bruce and Goldberg, 1985; Schall and Thompson, 1999) for both ipsilateral and contralateral saccades (Lawrence et al., 2005), similar to the spatially-dependent activity we observed in rat FOF neurons (Figures 3 and 4). In typical visual-guided saccade tasks a substantial portion of FEF neurons show responses to the onset of the stimulus (c.f. Schall et al., 1995), which we did not observe in our auditory-stimulus task. However, monkey FEF neurons also encode saccade vectors preceding auditory-guided saccades (Russo and Bruce, 1994), and show very little auditory-stimulus-driven activity. This again is similar to our observations in rat FOF (Figure 4AB). We note that although we have focused here on similarities to the monkey FEF, which is a particularly well-studied brain area, we do not believe we have established a strict homology between rat FOF and monkey FEF. Similarities to other cortical motor structures may be greater, or it may be that the rat FOF will not have a strict homology with any one primate cortical area.

We are aware of only one other electrophysiological study in rats during a memory-guided orienting task in which rats stay still during the delay period (Gage et al., 2010). In that study, Gage et al. recorded from M1, striatum, and globus pallidus. They found that, although a few response-selective signals in M1 could be observed many hundreds of milliseconds before the Go signal, maintained response selectivity in M1 neurons arose only ~180 ms before the Go signal. In contrast, once neurons of the FOF start firing in a response-selective manner, they usually maintain their response selectivity throughout the rest of the delay period (Figure 3), even when their response selectivity arises many hundreds of milliseconds before the Go signal. The population count of response selective FOF cells therefore starts rising very shortly after the end of the instruction signal, and rises continually until the Go signal (Figure 4F; compare to Figure 5B, top panel, of Gage et al., 2010). This suggests that orienting preparation signals are represented significantly earlier in the FOF than in M1. Consistent with the much weaker electrophysiological delay period signature found in M1, as compared to the FOF, unilateral pharmacological inactivations of

M1 produced very different, and much weaker, behavioral effects than those found in FOF (Figure S2, compare to Figure 2). The difference is particularly strong for memory trials. FOF inactivation reduced contralateral memory trials to almost 50% correct performance (chance), but M1 inactivation impaired performance on these trials only to ~75% correct. This was a saturated effect: doubling the dose of muscimol in M1 did not further impair performance (Figure S2). Much further work is required to draw and refine functional maps of the rat cortex during awake behaviors, but we do conclude that the role of the FOF in memory-guided orienting is not common across frontal motor cortex.

We targeted the FOF based on previous anatomical, lesion, and microstimulation studies that suggested a role for this area in orienting behaviors (Leonard, 1969; Cowey and Bozek, 1974; Crowne and Pathria, 1982; Sinnamon and Galer, 1984; Corwin and Reep, 1998). However, a different line of research, observing whisker movements in response to intracortical microstimulation in head-fixed, anesthetized rats, has described the same area as whisker motor cortex (Brecht et al., 2004). Nevertheless, the functional role of the FOF in awake animals is not firmly established: single-unit recordings from the area in awake animals remain very sparse (Carvell et al., 1996; Kleinfeld et al., 2002; Mizumori et al., 2005). We asked whether whisking played a role in our memory-guided orienting task, and found that it did not: removing the whiskers had little effect on performance (Figure 1D,F and associated text), unilaterally paralyzing the whiskers did not produce a lateralized or memory specific effect (Figure 1E,F), and video analysis of regular trials did not find evidence of asymmetric or lateralized whisking during the memory delay period. The video showed instead that whiskers are held quite still during the delay period (Figure S1 and Movie S2). We speculate that well-trained animals that are highly familiar with the spatial layout of the behavior apparatus do not use whisking to guide their movements during the task. In particular, whisking appears to play no role in the short-term memory component of the task (Movie S2). The lack of whisker-related effects on task performance or task behavior contrasts with the strong pharmacological and electrophysiological correlates with behavior that form the basis of this report, and suggests that the FOF plays a role in orienting that is independent from any role in control of whisking. Previous single-unit studies of this area in awake animals, focusing on whisker motor control, have suggested that the FOF is not primarily involved in low-level motor control of whisking, but may instead play a more prominent role in longer timescale (~ 1 sec or longer) control of whisking parameters (Carvell et al., 1996). More recent studies (D. Kleinfeld, personal communication) have identified some of the long timescale parameters as control of amplitude and offset angle of whisking; this last refers to the average orientation of the whiskers with respect to the head. Our data, by providing evidence that the FOF participates in the preparation of orienting movements many hundreds of milliseconds before these movements actually occur, is consistent with this view of the FOF as a high-level motor control area.

A third line of research in this cortical area, represented so far only by a book chapter (Mizumori et al., 2005), has described finding head direction cells (Taube, 2007) in the FOF. Our recordings replicated this finding (Figure S6). We found no correlation between the strength of a neuron's head direction tuning and the strength of its preparatory orienting signals (data not shown). The two types of signals coexist in the FOF, but are distinct from each other: a quantitative analysis showed that head direction tuning could not account for the preparatory orienting signals recorded during the delay period of memory trials (Figure 7). We found that head direction signals in the FOF are strongly modulated by behavioral context. That is, for many cells, tuning while animals were performing the task was very different to tuning while animals were not performing the task (Figure S6). The relationship between orienting preparation signals and head direction signals in the FOF is complex, and we will explore it in detail in a future manuscript.

The confluence of three different types of signals (orienting, head direction, whisking) in a single area is remarkable. Although different, the signals are related: head direction information is important for making orienting decisions, whisking reaps information from the environment that can then be used to guide orienting decisions, and orienting movements themselves will have a direct effect on both head direction and whisker position. Having these three signals represented in a single area is consistent with the view of the FOF as an area that integrates multiple sources of information in the service of high-level control of spatial behavior. Elucidating the precise relationship between these signals, both in the FOF and in other brain areas, will require many further experiments that will bring together the orienting, navigation, and whisking literatures.

EXPERIMENTAL PROCEDURES

Subjects

Animal use procedures were approved by the Princeton University Institutional Animal Care and Use Committee and carried out in accordance with National Institutes of Health standards. All subjects were male Long-Evans rats (Taconic, NY). Rats were placed on a restricted water schedule to motivate them to work for water reward.

Behavior

Rats went through several stages of an automated training protocol before performing the task as described in the results. (See Supplementary Experimental Procedures). All data described in this paper were collected from fully trained rats. Sessions with poor performance (<70% correct overall or fewer than 8 correct memory trials on each side without fixation violations) were excluded from analyses. These sessions were rare (2.4% of all sessions from trained rats) and were usually caused by problems with the hardware (e.g. a clogged water-reward valve or a dirty IR-photodetector).

To generate psychometric curves, we collected 12 data points: the % “Went Right” for each of 6 different click rates, separately for memory and for non-memory trials. We then combined the data points across all sessions (total data points per fit = 6 x # of sessions) and used Matlab’s `nlinfit.m` to fit a 4-parameter sigmoid to the data. For these fits, x is the natural logarithm of clicks/sec, y is “% Went Right”, and the four parameters to be fit are: x_0 , the inflection point of the sigmoid, b , the slope of the sigmoid, y_0 , the minimum “% Went Right”, and $a+y_0$ is the maximum “% Went Right”.

$$y = y_0 + \frac{a}{1 + e^{-\frac{(x-x_0)}{b}}}$$

Data from memory and non-memory trials were fit separately.

Surgery

All surgeries were done under isoflurane anesthesia (1.5-2%) using standard stereotaxic technique (See Supplementary Experimental Procedures for details). The target of all FOF surgeries in our Long-Evans strain rats was +2 AP, ±1.3 ML (mm from Bregma). This location was chosen because it was the center of the distribution of stimulation sites that resulted in contralateral orienting movement in Sinnamon & Galer (1984).

Infusions

Dose and volume of muscimol infusions into FOF was 0.5 mg/mL and 0.3 μ L respectively. Infusions for M1 were done in two sets of experiments, first 0.5 mg/mL and 0.3 μ L, then 1 mg/mL and 0.3 μ L. See Supplementary Experimental Procedures for details.

Recordings

Recordings were made with platinum iridium wire (16.66 μ m, California Fine Wire, CA) twisted into tetrodes. Wires were gold-plated to 0.5-1.2 MOhm. Spike sorting was done by hand using SpikeSort3D (Neuralynx). Cells had to satisfy several criteria to be included in the presented analyses: 1) Zero inter-spike intervals < 1 ms; 2) Signal to noise ratio > 4; 3) At least one timepoint of a smoothed, response-aligned PETH had to have a firing rate of at least 3 spikes/sec. We recorded 378 cells over 100 sessions that satisfied the 1st two criteria. 242 cells (recorded from 91 sessions) satisfied all 3 criteria. Median number of cells per session was three. The maximum number of cells recorded in a session was eleven.

Neural Data Analysis

We examined a 2 second window around the Go signal (−1.5s pre, to +0.5s post). Spikes from each trial were smoothed with a causal half-gaussian kernel with a full-width s.d. of 200 ms--that is, the firing rate reported at time t averages over spikes in an ~200 ms-long window preceding t . The resulting smooth traces were sampled every 10 ms. To determine whether cells were response-selective at any point between the stimulus and the rat's choice, we divided correctly performed trials into contralateral-orienting and ipsilateral-orienting groups, and used ROC analysis at each timepoint to ask whether the firing rates of the two groups were significantly different for that timepoint. For each cell, we randomly shuffled ipsi and contra trial labels 2000 times and recomputed ROC values. We labeled individual time bins as significant if fewer than 1% of the shuffles produced ROC values for that time bin that were further from chance (0.5) than the original data was (i.e., $p < 0.01$ for each time bin). We then counted the percentage of shuffles that produced a number of significant bins greater than or equal to the number of bins labeled significant in the original data. If this randomly produced percentage was less than 5%, the cell as a whole was labeled significant (i.e., an overall $p < 0.05$ for each cell).

To determine the time at which the population count of significant cells became greater than chance, we used binomial statistics. These indicate that with probability 0.999, at any given timepoint, an individual cell threshold of $p < 0.01$ would lead to fewer than 8/242 cells being labeled significant by chance. The population count was designated as significantly different from chance when it went above this $p < 0.001$ population threshold.

In order to quantify whether neurons in FOF tended to encode the stimulus or the response we generated a Stimulus Selectivity Index (SSI) from Go aligned PETHs for correct and error trials as follows:

$$SSI_{tt} = \frac{\sum_{t=-1.5}^{0.5} PETH_{contra,tt} - PETH_{ipsi,tt}}{\sum_{t=-1.5}^{0.5} PETH_{contra,tt} + PETH_{ipsi,tt}}$$

where tt indicates trial type (correct-memory, correct-non-memory, error-memory, and error-non-memory). If a cell fired only on contra and not on ipsi trials, then $SSI=1$. If a cell fired on ipsi and not contra trials, then $SSI=-1$. If a cell fired equally for ipsi and contra trials then $SSI=0$.

For latency estimations, we used an alignment algorithm to find a relative temporal offset for each trial as follows. Given a signal as a function of time for each trial (either firing rate or head angular velocity), we computed the trial-averaged signal. For each trial we then found the time of the peak of the cross-correlation function between the signal for that trial and the trial-averaged signal. We then shifted each trial accordingly, and recomputed the trial-averaged signal after. We iterated this process until the variance of the trial-averaged signal converged, typically within fewer than 5 iterations. The output of this alignment procedure was an offset time for each trial, which indicated the relative latency for that trial.

Histology

In all cases the electrode and cannula placements in FOF were within the borders of M2 and between 2 and 3 mm anterior to Bregma (Paxinos and Watson, 2004). In all cases the M1 placements were within the borders of M1 and between 2.5 and 3.5 mm anterior to Bregma (Paxinos and Watson, 2004).

Supplementary Material

Refer to Web version on PubMed Central for supplementary material.

Acknowledgments

We thank B.W. Brunton and J.K. Jun for contributions to software to obtain head direction data, D.W. Tank and J.P. Rickgauer for suggestions to improve whisker tracking, B.W. Brunton, J.K. Jun, C.D. Kopec, and T. Hanks for discussion and comments on the manuscript, A. Keller and D. Kleinfeld for discussions related to the role of the FOF in whisker control, and L. Osorio and G. Brown for technical assistance.

REFERENCES

- Arbib MA. From visual affordances in monkey parietal cortex to hippocampo-parietal interactions underlying rat navigation. *Philos Trans R Soc Lond B Biol Sci.* 1997; 352:1429–1436. [PubMed: 9368931]
- Bisley JW, Goldberg ME. Attention, intention, and priority in the parietal lobe. *Annu Rev Neurosci.* 2010; 33:1–21. [PubMed: 20192813]
- Brecht M, Krauss A, Muhammad S, Sinai-Esfahani L, Bellanca S, Margrie TW. Organization of rat vibrissa motor cortex and adjacent areas according to cytoarchitectonics, microstimulation, and intracellular stimulation of identified cells. *J Comp Neurol.* 2004; 479:360–373. [PubMed: 15514982]
- Britten KH, Newsome WT, Shadlen MN, Celebrini S, Movshon JA. A relationship between behavioral choice and the visual responses of neurons in macaque MT. *Vis Neurosci.* 1996; 13:87–100. [PubMed: 8730992]
- Bruce CJ, Goldberg ME. Primate frontal eye fields. I. Single neurons discharging before saccades. *J Neurophysiol.* 1985; 53:603–635. [PubMed: 3981231]
- Bruce CJ, Goldberg ME, Bushnell MC, Stanton GB. Primate frontal eye fields. II. Physiological and anatomical correlates of electrically evoked eye movements. *J Neurophysiol.* 1985; 54:714–734. [PubMed: 4045546]
- Carvell GE, Miller SA, Simons DJ. The relationship of vibrissal motor cortex unit activity to whisking in the awake rat. *Somatosens Mot Res.* 1996; 13:115–127. [PubMed: 8844960]
- Conde F, Maire-Lepoivre E, Audinat E, Crepel F. Afferent connections of the medial frontal cortex of the rat. II. Cortical and subcortical afferents. *J Comp Neurol.* 1995; 352:567–593. [PubMed: 7722001]
- Corwin JV, Reep RL. Rodent posterior parietal cortex as a component of a cortical network mediating directed spatial attention. *Psychobiology.* 1998; 26:87–102.
- Cowey A, Bozek T. Contralateral ‘neglect’ after unilateral dorsomedial prefrontal lesions in rats. *Brain Res.* 1974; 72:53–63. [PubMed: 4830476]

- Crowne DP, Pathria MN. Some attentional effects of unilateral frontal lesions in the rat. *Behav Brain Res.* 1982; 6:25–39. [PubMed: 7126323]
- Crowne DP, Richardson CM, Dawson KA. Parietal and frontal eye field neglect in the rat. *Behav Brain Res.* 1986; 22:227–231. [PubMed: 3790245]
- Curtis CE, Connolly JD. Saccade preparation signals in the human frontal and parietal cortices. *J Neurophysiol.* 2008; 99:133–145. [PubMed: 18032565]
- Dias EC, Segraves MA. Muscimol-induced inactivation of monkey frontal eye field: effects on visually and memory-guided saccades. *J Neurophysiol.* 1999; 81:2191–2214. [PubMed: 10322059]
- Donoghue JP, Wise SP. The motor cortex of the rat: cytoarchitecture and microstimulation mapping. *J Comp Neurol.* 1982; 212:76–88. [PubMed: 6294151]
- Dorris MC, Munoz DP. Saccadic probability influences motor preparation signals and time to saccadic initiation. *J Neurosci.* 1998; 18:7015–7026. [PubMed: 9712670]
- Felsen G, Mainen ZF. Neural substrates of sensory-guided locomotor decisions in the rat superior colliculus. *Neuron.* 2008; 60:137–148. [PubMed: 18940594]
- Ferrier D. Experiments on the Brain of Monkeys. No. 1. P. R. Soc. 1875; xxiii:409–430.
- Funahashi S, Bruce CJ, Goldman-Rakic PS. Neuronal activity related to saccadic eye movements in the monkey's dorsolateral prefrontal cortex. *J Neurophysiol.* 1991; 65:1464–1483. [PubMed: 1875255]
- Fuster JM. The prefrontal cortex and its relation to behavior. *Prog Brain Res.* 1991; 87:201–211. [PubMed: 1907745]
- Gage GJ, Stoetzer CR, Wiltschko AB, Berke JD. Selective activation of striatal fast-spiking interneurons during choice execution. *Neuron.* 2010; 67:466–479. [PubMed: 20696383]
- Glimcher PW. The neurobiology of visual-saccadic decision making. *Annu Rev Neurosci.* 2003; 26:133–179. [PubMed: 14527268]
- Gold JI, Shadlen MN. Neural computations that underlie decisions about sensory stimuli. *Trends Cogn Sci.* 2001; 5:10–16. [PubMed: 11164731]
- Goldman-Rakic PS, Bates JF, Chafee MV. The prefrontal cortex and internally generated motor acts. *Curr Opin Neurobiol.* 1992; 2:830–835. [PubMed: 1477547]
- Green, DM.; Swets, JA. Signal detection theory and psychophysics. R. E. Krieger Pub. Co; Huntington, N.Y.: 1974.
- Guandalini P. The corticocortical projections of the physiologically defined eye field in the rat medial frontal cortex. *Brain Res Bull.* 1998; 47:377–385. [PubMed: 9886790]
- Hebb DO, Penfield W. Human behavior after extensive bilateral removal from the frontal lobes. *Archives of Neurology and Psychiatry.* 1940; 44:421–438.
- Hull CL. The goal gradient hypothesis and maze learning. *Psychol Rev.* 1932; 39:25–43.
- Kargo WJ, Szatmary B, Nitz DA. Adaptation of prefrontal cortical firing patterns and their fidelity to changes in action-reward contingencies. *J Neurosci.* 2007; 27:3548–3559. [PubMed: 17392471]
- Keller EL, Lee KM, Park SW, Hill JA. Effect of inactivation of the cortical frontal eye field on saccades generated in a choice response paradigm. *J Neurophysiol.* 2008; 100:2726–2737. [PubMed: 18784274]
- Kleinfeld D, Ahissar E, Diamond ME. Active sensation: insights from the rodent vibrissa sensorimotor system. *Curr Opin Neurobiol.* 2006; 16:435–444. [PubMed: 16837190]
- Kleinfeld D, Sachdev RN, Merchant LM, Jarvis MR, Ebner FF. Adaptive filtering of vibrissa input in motor cortex of rat. *Neuron.* 2002; 34:1021–1034. [PubMed: 12086648]
- Knudsen EI, Cohen YE, Masino T. Characterization of a forebrain gaze field in the archistriatum of the barn owl: microstimulation and anatomical connections. *J Neurosci.* 1995; 15:5139–5151. [PubMed: 7623141]
- Kunzle H, Akert K, Wurtz RH. Projection of area 8 (frontal eye field) to superior colliculus in the monkey. An autoradiographic study. *Brain Res.* 1976; 117:487–492. [PubMed: 825196]
- Lawrence BM, White RL 3, Snyder LH. Delay-period activity in visual, visuomovement, and movement neurons in the frontal eye field. *J Neurophysiol.* 2005; 94:1498–1508. [PubMed: 15843482]

- Leichnetz GR, Hardy SG, Carruth MK. Frontal projections to the region of the oculomotor complex in the rat: a retrograde and anterograde HRP study. *J Comp Neurol.* 1987; 263:387–399. [PubMed: 2822775]
- Leonard CM. The prefrontal cortex of the rat. I. Cortical projection of the mediodorsal nucleus. II. Efferent connections. *Brain Res.* 1969; 12:321–343. [PubMed: 4184997]
- McNaughton BL, Battaglia FP, Jensen O, Moser EI, Moser MB. Path integration and the neural basis of the ‘cognitive map’. *Nat Rev Neurosci.* 2006; 7:663–678. [PubMed: 16858394]
- Mishkin M, Pribram KH. Analysis of the effects of frontal lesions in monkey. 1. Variations of delayed alternation. *J Comp Physiol Psychol.* 1955; 48:492–495. [PubMed: 13271624]
- Mizumori, SJY.; Puryear, CB.; Gill, KK.; Guazzelli, A. Head direction codes in hippocampal afferent and efferent systems: What function do they serve?. In: Wiener, W.; Taube, JS., editors. *Head Direction Cells and the Neural Mechanisms Underlying Directional Orientation.* MIT Press; Cambridge: 2005. p. 203-220.
- Monteon JA, Constantin AG, Wang H, Martinez-Trujillo JC, Crawford JD. Electrical Stimulation of the Frontal Eye Fields in the Head-Free Macaque Evokes Kinematically Normal 3D Gaze Shifts. *J Neurophysiol.* 2010
- Moser EI, Kropff E, Moser MB. Place Cells, Grid Cells, and the Brain’s Spatial Representation System. *Annu Rev Neurosci.* 2008; 31:69–89. [PubMed: 18284371]
- Munoz DP, Wurtz RH. Role of the rostral superior colliculus in active visual fixation and execution of express saccades. *J Neurophysiol.* 1992; 67:1000–1002. [PubMed: 1588382]
- Nakamura K. Auditory spatial discriminatory and mnemonic neurons in rat posterior parietal cortex. *J Neurophysiol.* 1999; 82:2503–2517. [PubMed: 10561422]
- Narayanan NS, Laubach M. Top-down control of motor cortex ensembles by dorsomedial prefrontal cortex. *Neuron.* 2006; 52:921–931. [PubMed: 17145511]
- Neafsey EJ, Bold EL, Haas G, Hurley-Gius KM, Quirk G, Sievert CF, Terreberry RR. The organization of the rat motor cortex: a microstimulation mapping study. *Brain Res.* 1986; 396:77–96. [PubMed: 3708387]
- Olton DS, Samuelson RJ. Remembrance of Places Passed - Spatial Memory in Rats. *J Exp Psychol Anim Behav Process.* 1976; 2:97–116.
- Paxinos, G.; Watson, C. *The Rat Brain in Stereotaxic Coordinates.* Elsevier; New York: 2004.
- Reep RL, Corwin JV. Posterior parietal cortex as part of a neural network for directed attention in rats. *Neurobiol Learn Mem.* 2009; 91:104–113. [PubMed: 18824116]
- Reep RL, Corwin JV, Hashimoto A, Watson RT. Afferent connections of medial precentral cortex in the rat. *Neurosci Lett.* 1984; 44:247–252. [PubMed: 6728294]
- Reep RL, Corwin JV, Hashimoto A, Watson RT. Efferent connections of the rostral portion of medial agranular cortex in rats. *Brain Res Bull.* 1987; 19:203–221. [PubMed: 2822206]
- Riehle A, Requin J. The predictive value for performance speed of preparatory changes in neuronal activity of the monkey motor and premotor cortex. *Behav Brain Res.* 1993; 53:35–49. [PubMed: 8466666]
- Russo GS, Bruce CJ. Frontal eye field activity preceding aurally guided saccades. *J Neurophysiol.* 1994; 71:1250–1253. [PubMed: 8201415]
- Schall JD. Neural basis of deciding, choosing and acting. *Nat Rev Neurosci.* 2001; 2:33–42. [PubMed: 11253357]
- Schall JD, Thompson KG. Neural selection and control of visually guided eye movements. *Annu Rev Neurosci.* 1999; 22:241–259. [PubMed: 10202539]
- Schall JD, Morel A, King DJ, Bullier J. Topography of visual cortex connections with frontal eye field in macaque: convergence and segregation of processing streams. *J Neurosci.* 1995; 15:4464–4487. [PubMed: 7540675]
- Schiller PH, Tehovnik EJ. Neural mechanisms underlying target selection with saccadic eye movements. *Prog Brain Res.* 2005; 149:157–171. [PubMed: 16226583]
- Sinnamon HM, Galer BS. Head movements elicited by electrical stimulation of the anteromedial cortex of the rat. *Physiol Behav.* 1984; 33:185–190. [PubMed: 6505061]

- Sommer MA, Tehovnik EJ. Reversible inactivation of macaque frontal eye field. *Exp Brain Res.* 1997; 116:229–249. [PubMed: 9348123]
- Steinmetz NA, Moore T. Changes in the response rate and response variability of area V4 neurons during the preparation of saccadic eye movements. *J Neurophysiol.* 2010; 103:1171–1178. [PubMed: 20018834]
- Stuesse SL, Newman DB. Projections from the medial agranular cortex to brain stem visuomotor centers in rats. *Exp Brain Res.* 1990; 80:532–544. [PubMed: 1696906]
- Taube JS. The head direction signal: origins and sensory-motor integration. *Annu Rev Neurosci.* 2007; 30:181–207. [PubMed: 17341158]
- Thompson KG, Biscoe KL, Sato TR. Neuronal basis of covert spatial attention in the frontal eye field. *J Neurosci.* 2005; 25:9479–9487. [PubMed: 16221858]
- Tolman EC. The determiners of behavior at a choice point. *Psychol Rev.* 1938; 45:1–41.
- Whitlock JR, Sutherland RJ, Witter MP, Moser MB, Moser EI. Navigating from hippocampus to parietal cortex. *Proc Natl Acad Sci U S A.* 2008; 105:14755–14762. [PubMed: 18812502]
- Zilles, KJ. *The cortex of the rat: A stereotaxic atlas.* Springer-Verlag; Berlin: 1985.

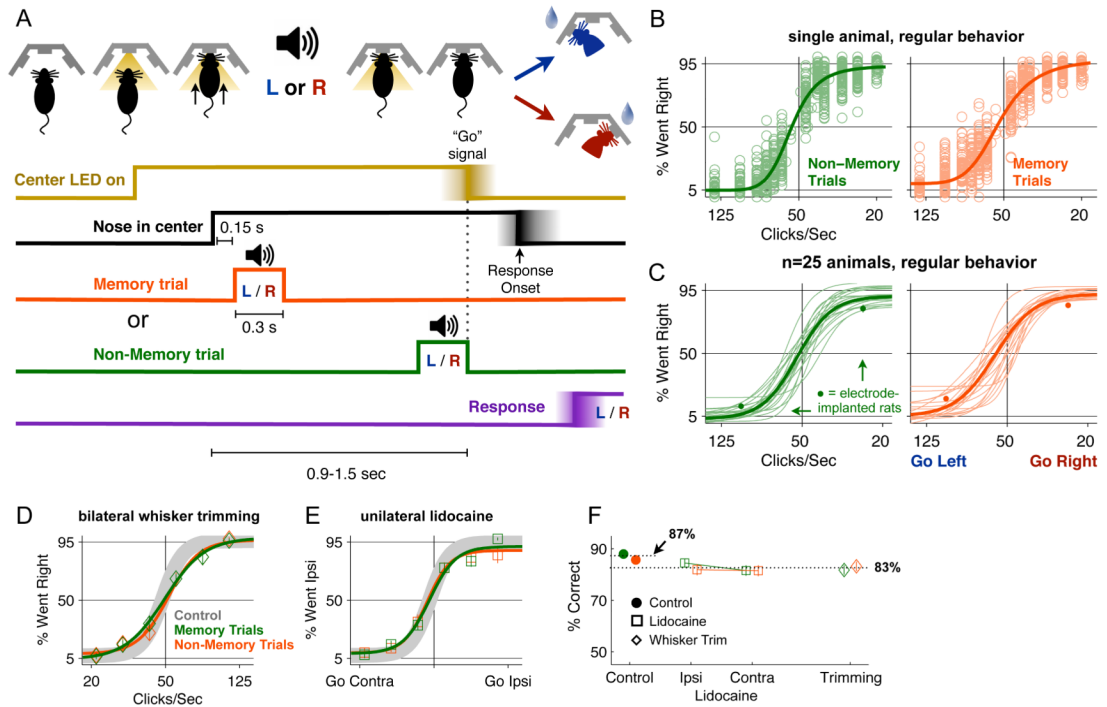


Figure 1. Memory-guided Frequency Discrimination Task and Behavioral Performance

(A) Task schematic, showing a cartoon of a rat in the behavior box and the timing of the events in the task. Onset of the Center LED indicated to the rat it should put its nose in the center port, and remain there until the LED was turned off. During this variable-duration “nose fixation” or “nose-in-center” period, a 300 ms-long periodic train of auditory clicks was played. Click rates higher than 50 clicks/sec indicated that a water reward would be available from the left port; click rates lower than 50 clicks/sec indicated reward would be available from the right port. On memory trials (orange), the click train was played near the beginning of the fixation period, and there was a several hundred ms delay between the end of the click train and the end of the nose fixation signal. On non-memory trials (green) the click train ended at the same time as the nose fixation signal. (B) An example of performance data for a single rat. Each circle indicates the percentage of trials in which the subject chose the right port for a given stimulus in a single session. There were 6 stimuli presented in each session. The thick line shows the psychometric curve, drawn as a 4-parameter sigmoidal fit to the circles. The left panel shows data from non-memory trials, and the right panel shows data from memory trials. (C) Psychometric curves showing performance of 20 rats. Thin lines are the fits to individual rats, as in panel B. Thick lines are the fits to the data combined across rats. The performance of electrode implanted rats ($n=5$) is shown by the small filled circles at the two stimuli used with these animals (25 clicks/sec and 100 clicks/sec). (D) Bilateral whisker trimming (3 rats) has a minimal effect on performance. The grey line is the average of memory and non-memory trials for control sessions before whisker trimming. Diamonds are data after trimming, solid lines are sigmoid fits. Memory trials are in orange, non-memory trials in green. (E) Unilateral whisker pad anesthesia and paralysis (4 rats) also has a minimal effect on performance. Open circles are data from lidocaine sessions. Color conventions as in panel D. (F) Summary of effects of whisker trimming and lidocaine (See also Figure S1, Movies S1-3).

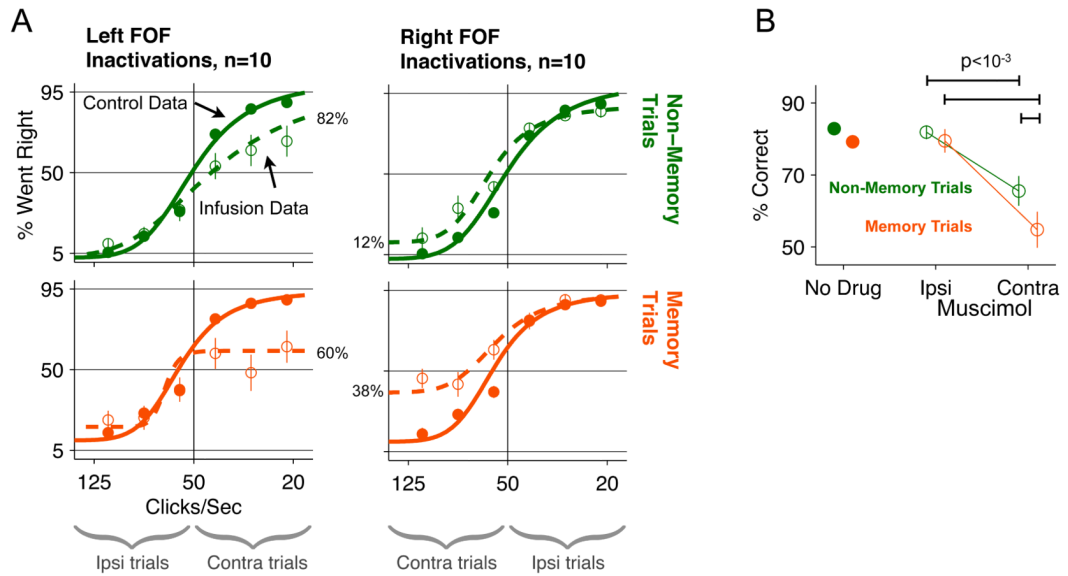


Figure 2. Unilateral inactivation of FOF generates a contralateral impairment that is larger for memory trials compared to non-memory trials

(A) Behavioral performance on control and muscimol-infusion days. Top row: non-memory trials. Bottom row: memory trials. Left column: muscimol infusions into left FOF. Right column: muscimol infusions into right FOF. Open circles, data from muscimol infusions. Closed circles: control data from days immediately preceding infusion days. Dashed lines: sigmoidal fits to muscimol data. Solid Lines: sigmoidal fits to control data. Error bars are standard error of the mean. Error bars for control data were smaller than the marker in most cases. Underbraces at bottom indicate the sets of trials in which animals were instructed to orient ipsilaterally or contralaterally to the site of infusion. The percentages aligned to the dashed curves indicate the endpoint performance for the trials contralateral to the infusion. (B) Combined data from left and right infusion sessions and collapsed across all stimulus difficulty levels. The “No Drug” data come from the 20 sessions one day before infusion sessions. The Ipsi and Contra Muscimol data are the performance on ipsilateral trials and contralateral trials on infusion sessions (n=20). (See also Figure S2)

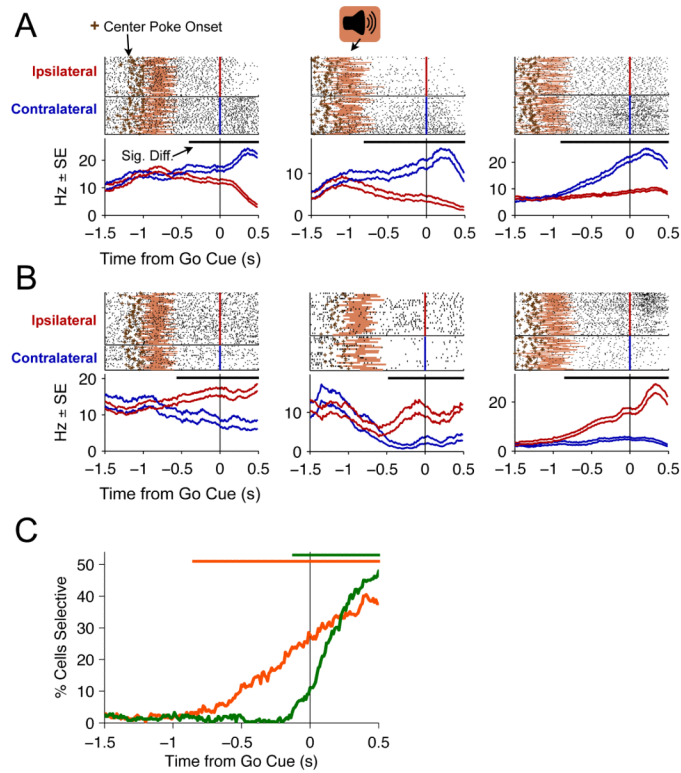


Figure 3. Upcoming choice-dependent delay period activity in the FOF

(A) Three contralateral preferring cells and (B) three ipsilateral preferring cells that show delay period activity that is dependent on the upcoming side choice. The top half of each panel shows spike rasters sorted by the side of the rat's response and aligned to the time of the Go cue. The pink shading indicates the time, for each trial, when the stimulus was on. The brown "+" indicates the time at which the rat placed its nose in the center port. The bottom half of each panel are PETHs of the rasters for ipsilateral (red) and contralateral (blue) trials. The two lines indicate the mean \pm std. err. PETHs were generated using a causal half-gaussian kernel with an S.D. of 200 ms. The thick black bar just below the rasters indicates the times when the cells response was significantly different on ipsi- vs contralateral trials ($p < 0.01$, ROC analysis). (C) Development of choice-dependent activity over the course of the trial. The lines indicate the % of cells (out of 242 neurons) that have significantly choice-dependent firing rate ($p < 0.01$) at each timepoint on memory trials (orange) and non-memory trials (green). (See Figure S3A,B for inter-spike interval histograms and waveforms for the example neurons)

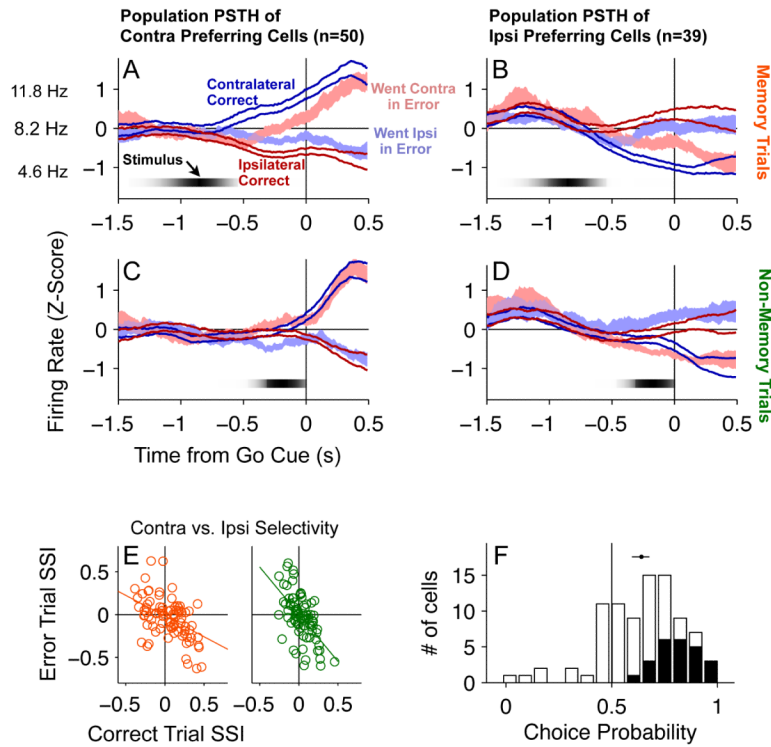


Figure 4. Predictive coding of contra- and ipsilateral choice in the FOF

(A-D) Each panel is a population PETH showing the average z-score normalized response on correct (thick lines, mean \pm s.e. across neurons) and error trials (shaded, mean \pm s.e. across neurons) where the correct response was contralateral (blue) or ipsilateral (red) to the recorded neuron. PETHs are aligned to the time of the ‘Go’ signal (center LED offset). (A) The average responses of memory trials for 53 contra-preferring neurons. Vertical axis tick marks indicate z-score value. The average firing rate across all cells used for z-score normalization is shown next to the z=0 mark (8.2 spikes/sec). This overall mean \pm the across-cell average of the PETH standard deviation are shown at the z = \pm 1 marks. They indicate a typical firing rate modulation of 7.2 spikes/sec. (B) The average responses of memory trials of 43 ipsi-preferring neurons. (C) Same as A but for non-memory trials. (D) Same as B but for non-memory trials. (E) Cells encode the direction of the motor response, not the identity of the cue stimulus. Scatter plots of the Side-Selectivity Index for memory trials (orange) and non-memory trials (green) (n=89). (F) Histogram of the choice probability of neurons for trials where the rat was instructed to go in the cells’ preferred direction (n=89). The dot and line indicate the mean \pm 95% c.i. of the mean. Black bars indicate individually significant neurons. White bars indicate neurons that were not individually significant.

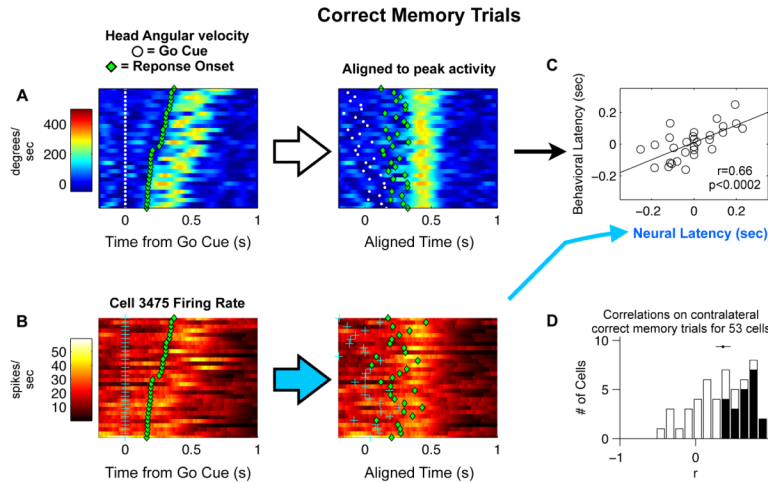


Figure 5. Trial-by-trial correlation of neural and behavioral latency

(A) Head angular velocity data from left correct memory trials in a single session. Each row is a single trial, showing head angular velocity (color-coded) as a function of time. The white dots indicate the time of the Go cue, and the green dots indicate the Response Onset time. Left panel: Trials are sorted by reaction time (Response Onset - Go cue). Right panel: same trials, after each trial has been time-shifted to maximize the similarity between the trial's angular velocity profile and the average of all the other trials. (B) Same trials as in panel A, but color code here indicates firing rate of a single neuron. Left panel is before alignment. Right panel is after time-alignment to maximize the similarity between each trial's firing rate profile and the average of all the other trials. (C) Correlation between the angular velocity time offsets and the neural firing rate time offsets computed in A&B. (D) Histogram of r values for 53 cells with significant delay period activity that were recorded during sessions where head-tracking was also recorded. Black bars indicate individual cells with correlations significantly greater than zero. The dot with the line through it shows the mean \pm s.e. of r values for the population. (See also Figure S5)

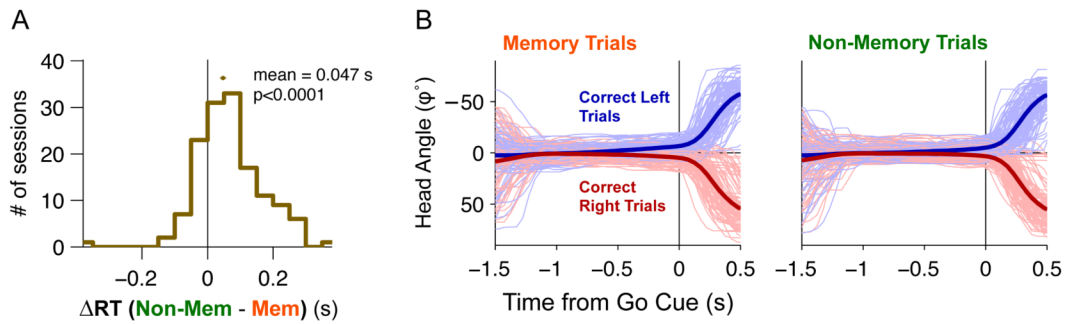


Figure 6. Rats plan their response during the delay period on memory trials

(A) Movement times (MT) are faster for memory trials than non-memory trials. Movement times are measured as median Response time - Response Onset time for each physiology session. The mean difference between memory and non-memory trials is 47 ms (t -test, $t_{141}=3.58$, $p < 10^{-5}$ from the 5 electrode implanted rats). The dot above the histogram indicates the mean \pm s.e. of the distribution. (B) Average head-angle data from 84 recording sessions. Thin lines are 200 example trials randomly sub-sampled from all 84 sessions. The thick lines are the average across all trials across all sessions. In our coordinate system, $\phi =$ zero degrees points directly towards the center port, positive ϕ corresponds to rightward orientations, and negative ϕ to left-ward orientations. On memory trials one can observe a subtle but clear change in the head angle in the direction of the response during the delay period, starting around 500 ms before the end of the fixation period. (See also Figure S6 for head-direction related neural activity)

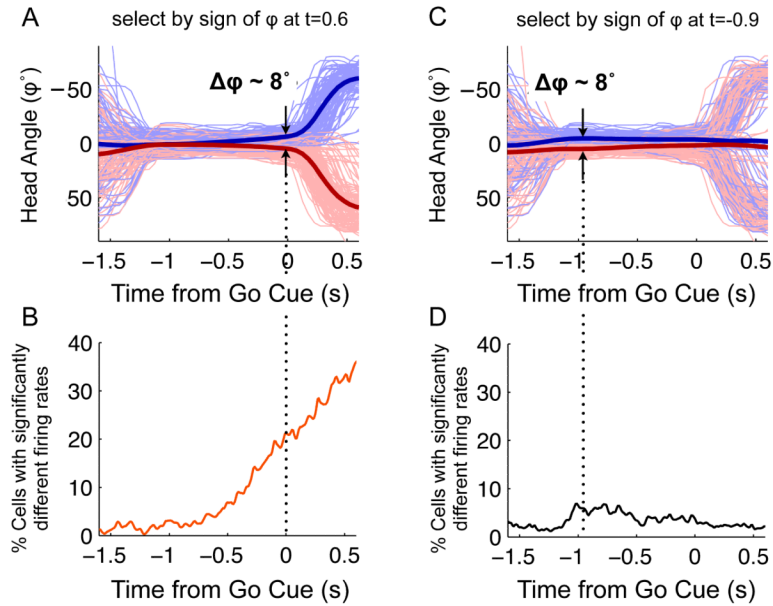


Figure 7. Predictive coding of response is not a simple function of current head angle
A, C Plots of head angle as a function of time relative to the Go signal for memory trials. Thin blue lines are from a random subsample of trials where the head angle was greater than 0 (oriented leftwards from center port) at the time indicated by the vertical dotted line; thin red lines are from a random subsample of trials where the head angle was less than 0 at the indicated time: $t=+0.6$ sec for **A** and $t=-0.9$ sec for **C**, relative to the Go signal. Thick lines are the mean head angles for each group, averaged over all correct memory trials. **B**, ROC plot (similar to 5b) for the trial grouping defined in **A**. **D**, ROC plot for the trial grouping defined in **C**. (See Figure S7 for similar analyses using angular velocity and acceleration).